ФИЗИКА

УДК 538.91:541.65/.654 DOI: https://doi.org/10.54341/20778708_2023_1_54_60
EDN: PYOQLH

ПОЛУЧЕНИЕ ПОЛЫХ СФЕР CuS, ЛЕГИРОВАННЫХ Zn^{2+}, ПУТЕМ ОДНОСТАДИЙНОГО СИНТЕЗА И ЕГО ФОТОКАТАЛИТИЧЕСКИЕ СВОЙСТВА В ВИДИМОМ СВЕТЕ

Гаопэн Ян[1], Тяньтянь Ву[1], Цзиньсин Цао[2], Сяохун Цзян[1]

[1]*Нанкинский университет науки и технологий*
[2]*Нанкинский университет Сяочжуан*

PREPARATION OF Zn^{2+}-DOPED CuS HOLLOW SPHERES BY ONE-STEP SYNTHESIS AND ITS PHOTOCATALYTIC PERFORMANCE IN VISIBLE LIGHT

Gaopeng Yang[1], Tiantian Wu[1], Jinxing Cao[2], Xiaohong Jiang[1]

[1]*Nanjing University of Science and Technology*
[2]*Nanjing Xiaozhuang University*

Аннотация. В настоящее время фотокаталитические технологии очистки воды широко используются в зеленой энергетике и характеризуются высоким прикладным значением. Актуальным направлением в этой области является получение эффективных фотокатализаторов с помощью простых и экологически чистых способов. В этом исследовании предложен технологически простой, недорогой и экологически чистый метод получения CuS сфер легированных Zn^{2+}. Отличительной чертой данного метода является его одностадийность и низкая температура синтеза, позволяющая получить фотокализатор на основе CuS сфер с равномерно распределенными Zn^{2+} ионами. Морфология, структура и химический состав полученных продуктов исследованы растровой электронной и просвечивающей микроскопией, а также методами рентгеноструктурного анализа. Установлено, что введение Zn^{2+} в CuS приводит к образованию ловушек носителей заряда, которые ускоряют перенос электронов на поверхность катализатора, что значительно увеличивает скорость отклика на облучение видимым светом, но при этом снижается скорость рекомбинации электронно-дырочных пар. С учетом большой удельной поверхности CuS сфер происходит рост количества поверхностно-активных адсорбирующих центров, что увеличивает эффективность фотокатализа. Установлено, что введение Zn^{2+} в CuS приводит к увеличению скорости катализа до 0,04736 $мин^{-1}$, что в 12 раз больше, в сравнении с нелегированным CuS.

Ключевые слова: *фотокатализ*, CuS, *полые сферы*, *видимое излучение*, Zn^{2+} *ионы*.

Для цитирования: *Получение полых сфер* CuS, *легированных* Zn^{2+}, *путем одностадийного синтеза и его фотокаталитические свойства в видимом свете* / Гаопэн Ян, Тяньтянь Ву, Цзиньсин Цао, Сяохун Цзян // Проблемы физики, математики и техники. – 2023. – № 1 (54). – С. 60–68. – DOI: https://doi.org/10.54341/20778708_2023_1_54_60. – EDN: PYOQLH

Abstract. At present, photocatalytic water treatment technology has important potential application value in the field of green energy. It is very attractive to prepare efficient photocatalysts by simple and green methods. In this study, a simple, low temperature, low cost and green low temperature water bath stirring method was designed to synthesize the well-dispersed Zn^{2+}-doped CuS hollow sphere photocatalyst in one step. The morphology, structure and composition of the obtained products were examined by field emission scanning electron microscopy, transmission electron microscopy and X-ray diffraction. Zn^{2+} doping forms carrier traps, which improve the transfer rate of electrons to the surface of the catalyst, significantly enhance its visible light response, and reduce the recombination rate of electron holes. Combined with the special interconnection channel and large specific surface area of the hollow sphere structure, it provides more surface active sites for adsorption and makes photocatalysis more efficient. The reaction rate of the prepared hollow spherical Zn^{2+}-doped CuS catalyst reached 0,04736 min^{-1}, which was 12 times that of pure CuS.

Keywords: *photocatalysis*, CuS, *hollow sphere*, *visible light*, Zn^{2+} *doped.*

For citation: *Preparation of* Zn^{2+}*-doped* CuS *hollow spheres by one-step synthesis and its photocatalytic performance in visible light* / Gaopeng Yang, Tiantian Wu, Jinxing Cao, Xiaohong Jiang // Problems of Physics, Mathematics and Technics. – 2023. – № 1 (54). – P. 60–68. – DOI: https://doi.org/10.54341/20778708_2023_1_54_60. – EDN: PYOQLH

Introduction

Due to the energy crisis and environmental pollution problems, photocatalytic treatment has attracted great interest as one of the most efficient and promising methods to eliminate organic and toxic pollutants in water [1]. To date, much attention has been paid to the development of novel, non-toxic and visible-light driven photocatalysts with high photocatalytic efficiency and stability [2]. Metal sulfide semiconductor is a promising candidate material for photocatalytic reactions. CuS is a very important metal sulfide semiconductor material with excellent photoelectric properties and is also considered as a typical P-type semiconductor material [3].

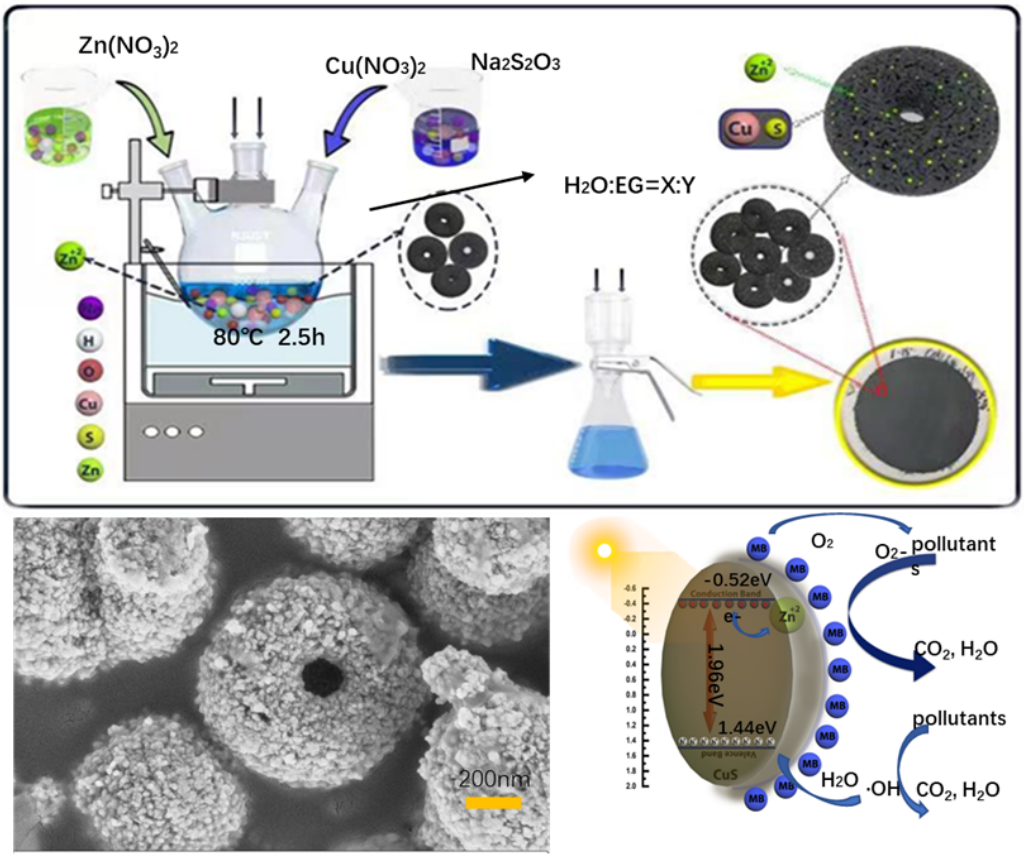

Figure 0.1

CuS is a narrow band gap semiconductor with a 2.2 eV forbidden bandwidth that exhibits many excellent physical and chemical characteristics and has great potential for applications such as solar cells, lithium battery electrodes, photothermal conversion, and photocatalysis [4]. CuS the forbidden band width of the narrow and has good visible light absorption, when the absorbed energy of the photons is right, CuS materials can produce light of electrons and holes, migration to the material surface, and the adsorption on the surface of the material, water or oxygen molecules reaction material, with high catalytic activity for degradation of material surface adsorption of organic matter [5]–[10]. However, CuS has the fatal disadvantages of poor electron hole pair generation ability and poor photocorrosion resistance, which also hinder its development in the field of photocatalysis [11]. Therefore, improving the photoactivity and photostability of CuS is a key problem and a major challenge in a wide range of practical applications [12].

1 Materials and method

In this work, we reported for the first time the one-step preparation of Zn^{2+}-doped CuS photocatalyst by using low-temperature water bath agitation instead of hydrothermal method. By adjusting the solvent ratio (water: Ethylene glycol = $x : y$), the effect of solvent on the morphology and photocatalytic performance of Zn^{2+}-doped CuS was studied. The performance of hollow spherical Zn^{2+}-doped CuS with solvent ratio of 3:1 (water: Ethylene glycol) was 12 times higher than that of plain pure CuS.

The Zn^{2+}-doped CuS photocatalyst was prepared by one-step low temperature water bath stirring method instead of complex and complicated hydrothermal method. Sodium thiosulfate as a sulfur source, copper nitrate as copper source, and 1mmol zinc nitrate together into 40 ml of a certain ratio of water and ethylene glycol mixture to form a yellow-green liquid, were put into a constant temperature water bath pot at a constant temperature of 80° C and stirred vigorously for 2,5 h. After the solution was cooled to room temperature, the black solid product was collected by filtration and then washed with absolute ethanol and deionized water and dried at 70° C for 6 hours for further characterization.

2 Results

2.1 *Morphological structure and phase*

The classical SEM (Zn^{2+}-doped CuS with the strongest catalytic activity) is shown in Figure 2.1, *b*. It can be clearly seen that we have synthesized the classical hollow spherical photocatalyst with a size of about 700 nm and formed by a large number of nanoparticles. The spherical surface also has pores (Figure 2.1, *c*), which makes it have a much higher specific surface area than the ordinary shape

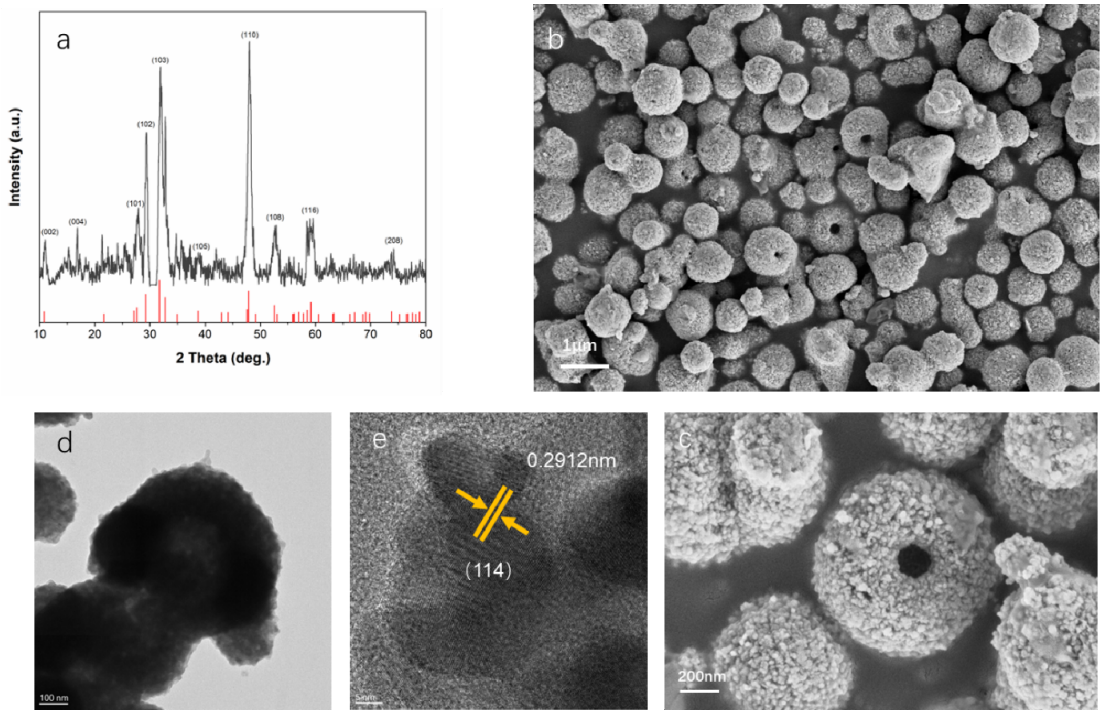

Figure 2.1 – XRD pattern of hollow sphere sample (*a*), SEM image(*b*, *c*), TEM (*d*), and HRTEM image (*d*) of hollow sphere sample

photocatalyst. The contact between the photocatalyst and the degradation material in the photocatalytic reaction is increased, and the photocatalytic performance is greatly improved. EDS spectra also confirmed that Zn^{2+} was doped into CuS. In addition, in transmission electron microscope Figure 2.1, *d*, we can see that the prepared Zn^{2+}-doped CuS photocatalysts are regular hollow spheres with hollow interior. From Figure 2.1, *e* we can observe clear lattice fringes, and the fringes with lattice spacing of 0,2913 nm correspond to the (114) crystal plane of CuS. The crystal structure and phase of the generated products were determined by XRD. The standard PDF card of CuS of hexagonal crystal was calibrated by red vertical line. It can be observed from Figure 2.1, *a* that the X-ray diffraction peak of the obtained product corresponded one to the peak of the standard PDF card of CuS of hexagonal crystal, and the diffraction peak of ZnS crystal was not observed. Therefore, combined with XPS and EDS test results, it can be verified that Zn^{2+} is successfully doped into the lattice defects of CuS in the form of ion doping.

2.2 *Chemical composition analysis*

The surface chemical state and elemental composition of Zn^{2+}-doped CuS were studied by XPS. The spectra were analyzed by Origin, as shown in Figure 2.2, *a*. The full spectrum of XPS binding energy indicates that the composite contains Cu, S, Zn and C elements and no other impurity signals are observed. The two peaks of 932,57 eV and 952,47 eV shown in the high-resolution spectrum of Cu2p in Figure 2.2, *b* are attributed to the binding energy of $Cu2p_{2/3}$ and $Cu2p_{1/2}$, respectively. According to the binding energy table of X-ray photoelectron spectrometer, the binding energy here represents the formation of CuS. Compared with the $Cu2p_{2/3}$ peak of pure CuS, the $Cu2p_{2/3}$ peak of Zn^{2+}-doped CuS has a slight blue shift (Figure 2.2, b). Combined with XRD, no diffraction peak of Zn metal compound can be found, indicating that Zn has been successfully doped into the surface of hexagonal CuS lattice. The S2p spectrum in Figure 2.2, *c* shows two peaks fitted at 163,3 eV and 162,3 eV, which belong to the sulfide in the CuS phase. The relative atomic content of Zn measured by MultiPak software is 1,9%, which is consistent with the results obtained by EDS spectroscopy. And a small amount of C element is the pollution carbon from the vacuum pump in the vacuum system of the XPS equipment [2], [13].

2.3 *Photocatalytic activity*

A xenon lamp with a power of 500 W was used as the light source, and a UV filter (K > 420 nm) was installed to simulate visible light. The photocatalytic performance of Zn^{2+}-doped CuS was evaluated at a room temperature. Methylene blue (MB) solution with a concentration of 30 mg/L was taken as the degradation object, and the 20 mg sample was dispersed in 50 ml MB solution. First, the adsorption was achieved in anamorphic chamber for 0,5 h to reach the balance of adsorption and desorption, and then the xenon lamp light source equipped with UV filter was irradiated for 2 hours to observe

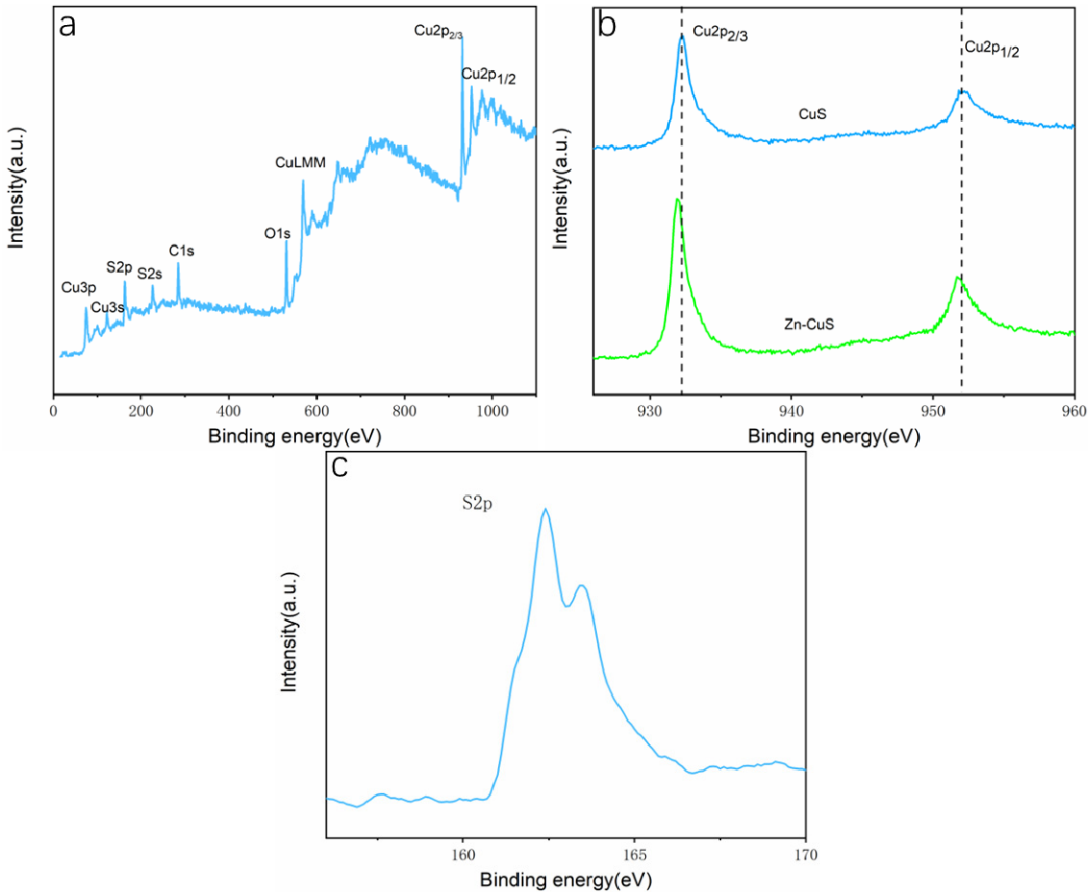

Figure 2.2 – XPS spectra of Zn^{2+}-doped CuS composites: (*a*) Survey; (*b*) Cu2p; (*c*) S2p

the degradation. It can be seen from Figure 2.3, *a* that the Zn^{2+}-doped CuS hollow sphere sample with solvent ratio of 3:1 has the best degradation effect, and the degradation efficiency reaches 100% after 1,5 hours of illumination. The photocatalytic rate reaction constant (Kapp) was obtained from the pseudo-first-order kinetic model: $-\ln(C / C0) = Kapp \cdot t$ [14]. As can be seen from Figure 2.3, *b*, the solvent ratio is 0:4, 1:3, 2:2, 3:1, 4 in the order of solvent ratio: The Kapp values of 0 and pure CuS were 0,00974 min^{-1}, 0,00157 min^{-1}, 0,0014 min^{-1}, 0,04581 min^{-1}, 0,0043 min^{-1} and 0,00421 min^{-1}, respectively. The hollow spherical sample is 12 times larger than the pure CuS sample. It is also superior to most reported CuS catalysts and has the potential to expand its application [15]–[17]. Photocatalysis is a heterogeneous reaction, so not only to refer to its energy band structure, morphology and specific surface area also have a profound impact on its photocatalytic effect [14], [18]. The large surface area and special multistage channels of Zn^{2+}-doped CuS hollow spheres are one of the reasons for their excellent photocatalytic performance. Moreover, the graded pores may reflect the incident light, which can make full use of light energy and enhance their photocatalytic performance. Considering that the stability of the photocatalytic material will affect the application, we conducted a cycle test on the sample. Figure 2.3, *c* shows that the photodegradation efficiency of the hollow spheres was 65,6% after five cycles (Figure 2.3, *c*). This is attributed to the consumption of photocatalyst during the recovery process. On the other hand, CuS has the problem of photocorrosion. We conducted XPS test on the cyclically degraded samples as shown in Figure 2.3, *d*. The peaks at 932,59 eV and 952,51 eV prove that the cyclically degraded samples are stable and still CuS.

2.4 *Adsorptive property, Energy band structure and Photocatalytic mechanism*

The surface area (Figure 2.4, *a*) and pore size (Figure 2.4, *b*) distribution of Zn^{2+}-doped CuS hollow sphere were studied by nitrogen sorption-desorption isotherm. The data of the hollow sphere is type IV isotherms, indicating that the sample has a mesoporous structure (2 – 50 nm). The sample has an H3 lag loop, which is related to the aggregation of nanoparticles (corresponding to SEM images). The aperture distribution maps obtained by the Barrett – Joyner - Halenda (BJH) method show only a single peak. The average pore sizes of the samples with the proportion of water in the solvent from 0 to 4 were 13,86 nm, 13,66 nm, 16,24 nm, 12,42 nm (hollow spherical sample) and 18,59 nm in Table 2.1, respectively.

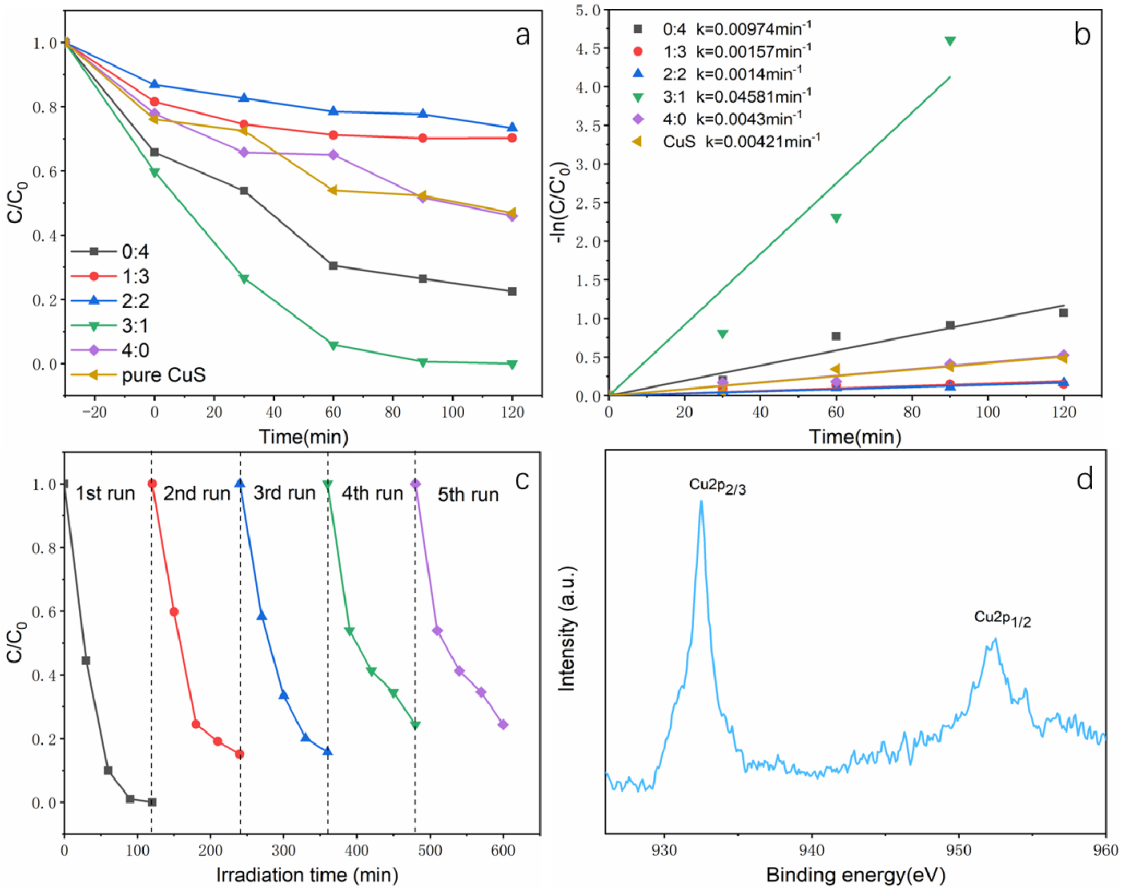

Figure 2.3 – (*a*) Photodegradation of MB (30 mg/L) by Zn^{2+} -doped CuS with different solvent ratio; (*b*) The corresponding kinetic curves of MB degradation by Zn^{2+} -doped CuS with different solvent ratio; (*c*) Cycling experiments of MB (30 mg/L) degradation by Zn^{2+} -doped CuS; (*d*) The high-resolution XPS spectrum of Zn^{2+} -doped CuS after the fourth photocycle

The corresponding specific surface areas were 7,85 m^2/g, 5,71 m^2/g, 7,28 m^2/g, 20,2 m^2/g (hollow spherical sample) and 2,9 m^2/g, respectively (Table 2.1). The specific surface area of the hollow spherical sample is 2.5 times, 3.5 times, 2.5 times and 7 times of the other samples in solvent ratio order, which may be due to the special interconnecting channels and graded pores of the hollow spherical structure.

Table 2.1

Medium	Morphology	Surface area (m^2g^{-1})	Pore volume (m^3g^{-1})	Eg (eV)
0:4	nano particles	7,85	0,04	1,85
1:3	nano particles	5,71	0,61	2,2
2:2	irregular shape	7,28	0,83	2,27
3:1	hollow sphere	20,2	0,94	1,96
4:0	sphere	2,9	0,12	1,76

Figure 2.4, *c* is the solid state ultraviolet (DRS) spectrum of the sample, showing the electronic states of Zn^{2+}-doped CuS samples generated by different solvents. Zn^{2+}-doped CuS samples have excellent absorption in the visible region, and the absorption curve has a red-shift trend compared with pure CuS samples. This is attributed to the doping of Zn^{2+} ions, which leads to an increase in the concentration of the hole-electron pair, making it easier to absorb the photon transition to the excited state, thus leading to a significant enhancement of its photoresponsive activity. The absorption spectra calculated by Kubelka-Munk theory show that the hollow spherical Zn^{2+}-doped CuS (water: glycol 3:1) with the best catalytic effect has the strongest absorption peak at 744 nm, and the strongest absorption peak of pure water and pure glycol as solvent are 662 nm and 738 nm, respectively. Both of them have good absorption of visible light. The absorption peaks of solvent ratio 1:3 and 2:2 have a significant red shift, and the wider absorption peaks are located in the near infrared (NIR) and infrared (IR) regions. According to the Kubelka-Munk function formula: $ahv = A\ (hv - Eg)^n$, the band gap [18], [19]. Where

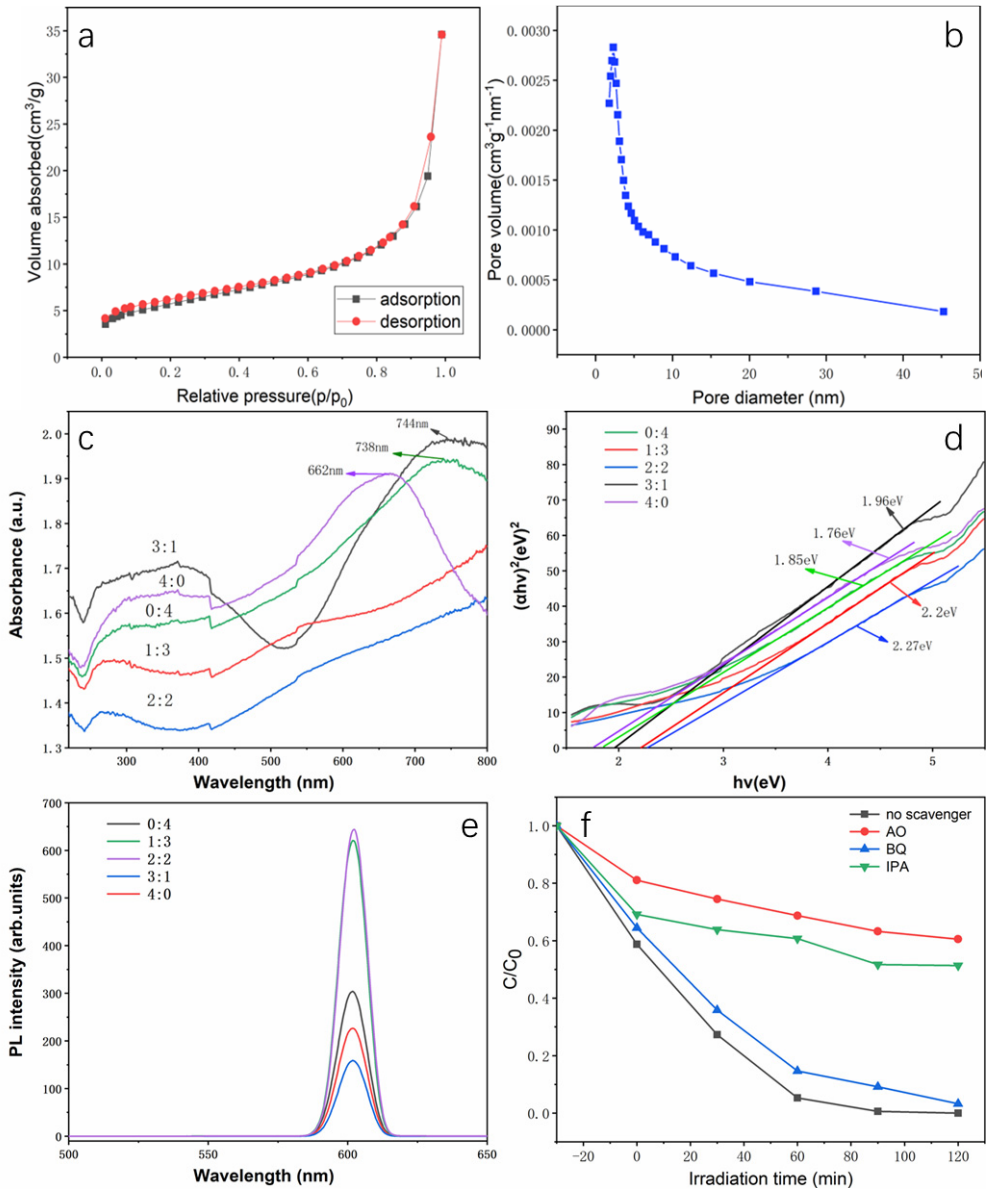

Figure 2.4 – (*a*) N_2 adsorption-desorption isotherm of Zn^{2+}-doped CuS
(*b*) Pore size distribution curve of Zn^{2+}-doped CuS,
(*c*) The DRS spectra of Zn^{2+}-doped CuS with different solvent ratio;
(*d*)The corresponding Tauc plots of Zn^{2+}-doped CuS with different solvent ratio,
(*e*) The PLspectra of Zn^{2+}-doped CuS with different solvent ratio,
(*f*) Effect of different scavengers on the degradation of MB (30 mg/L) by the hollow spheres Zn^{2+}-doped CuS under visible light conditions

Eg is the optical bandgap, A is A constant, and n = 1/2, 3/2, 2, or 3 depending on the nature of the electronic transition (1/2 for allowed direct transition, 2 for allowed indirect transition, 3/2 for forbidden direct transition, and 3 for forbidden indirect transition) [20]. Figure 2.4, *d* shows that the band gaps of the five gradient samples obtained by calculation are 1,85 eV, 2,2 eV, 2,27 eV, 1,96 eV and 1,76 eV (Table 2.1). The five different band gaps may be attributed to the quantum size effect of CuS and the Zn^{2+} doping concentration.

PL photoluminescence spectrum is also an important indicator to evaluate the photocatalytic performance of a material. PL is usually used to characterize material defects, including structural defects, inherent defects and non-inherent defects [21]. After the semiconductor absorbs light energy, when the energy absorbed is enough to change it from the ground state to the excited state, the electron will jump from the valence band to the conduction band. This creates an electron-hole pair [22]. And electrons and holes in the compound can make the photocatalytic properties, PL photoluminescence

spectrometer can through the electronic collection – hole in composite materials for electronic fluorescent information – hole pair recombination rate, peak intensity is proportional to the recombination rate, the lower the peak strength, material of electrons and holes, the lower the recombination rate, photocatalytic performance is better. It can be observed from Figure 2.4, *e* that the hollow sphere Zn^{2+}-doped CuS sample with the best performance has the lowest recombination rate, which may be attributed to its 1,9% Zn^{2+} doping concentration. Zn^{2+}-doped into the lattice of CuS forms lattice defects, which can be used as carrier traps, thus reducing the recombination rate of electron – hole pairs [23].

The conduction band and the valence band of a semiconductor are of great significance for the study of a photocatalytic mechanism. The band gap has been calculated by DRS, and the conduction band potential (ECB) and valence band potential (EVB) have been calculated by the following equation [24]

$$E_{VB} = \chi - E^e + 0,5E_g,$$

$$E_{CB} = E_{VB} - E_g.$$

Where *Eg* is the band gap energy of the semiconductor, Ee refers to the energy of the free electron on the hydrogen scale (about 4,5 eV), and χ is the geometric mean of the electronegativities of the constituent atoms, and the value of χ can be obtained from the following equation [25], [26]:

$$\chi = \left(x(A)^a \cdot x(B)^b \cdot x(C)^c\right)^{\frac{1}{a+b+c}},$$

where *a*, *b*, and *c* represent the number of atoms in the compound, χ(*A*), χ(*B*), and χ(*C*) refer to the absolute electronegativity of the corresponding atoms [27]. The calculated conduction band and valence band of Zn^{2+}-doped CuS are –0,52 eV and 1,44 eV, respectively.

According to the band gap, the conduction band and the valence band calculated above, we further analyzed the photocatalytic mechanism by a capture experiment. In the process of photocatalytic degradation, the main oxides involved in the reaction are hole (H+), hydroxyl radical (OH) and superoxide anion radical (O_{2-}). 2 mL ammonium oxalate monohydrate ($(COONH_4)_2 \cdot H_2O$, AO), benzoqui-none ($C_6H_4O_2$, BQ) and isopropanol (C_3H_8O) were used as scavengers of H+, O_{2-}, OH in the degradation process, respectively [28]. Figure 2.4, *f* shows the photocatalytic efficiency of Zn^{2+}-doped CuS hollow spherical catalyst in the presence of various scavengers. Compared with Zn^{2+}-doped CuS without scavenger, the degradation efficiency of Zn^{2+}-doped CuS with BQ scavenger has no significant effect, indicating that $\cdot O_{2-}$ does not play a key role in the photocatalytic process, which may be attributed to the doping of Zn ions providing more positions for charge recombination. The degradation efficiency of Zn^{2+}-doped CuS with AO and IPA decreased to 40% and 50%. These results indicate that h+ and OH play crucial roles in the photocatalytic process of Zn^{2+}-doped CuS. This may be attributed to the fact that Zn^{2+} ions doped on the lattice surface of CuS form carrier traps, which can promote the transfer of electrons to the interface of Zn^{2+}-doped CuS photocatalyst, thus improving the efficiency of hole extraction and greatly increasing the hole concentration, which plays a dominant role in the photocatalytic reaction process [23].

Through a series of characterization such as morphology, structure, band gap and photoluminescence, the differences of photocatalytic performance of Zn^{2+}-doped CuS were comprehensively discussed. Under a visible light irradiation, the photocatalytic efficiency of hollow spherical Zn^{2+} doped CuS samples is the best. After reaching adsorption equilibrium, the degradation efficiency reaches 100% in 90 min under light conditions. First of all, the hollow sphere has a special interconnecting channel and a hierarchical pore structure. The special structure makes it have the largest specific surface area among the five groups of samples, which can provide more surface active sites for adsorption, and the adsorption performance is particularly outstanding.

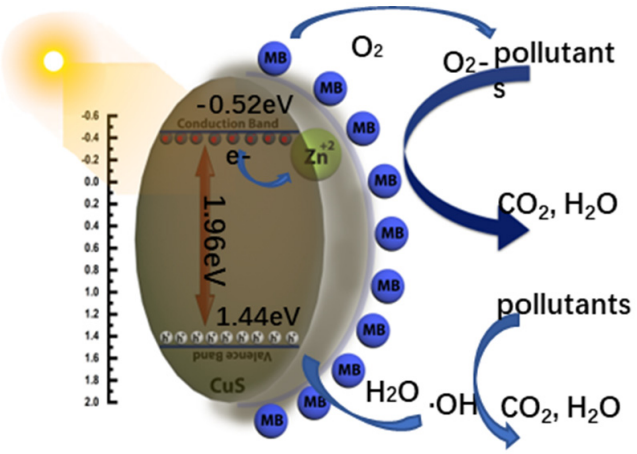

Figure 2.5 – Photocatalytic mechanism of Zn^{2+}-doped CuS hollow spheres under visible light

The light utilization efficiency of the catalyst is improved by scattering the incident light with special structure. The large specific surface area also makes the contact area between catalyst and pollutant in the process of photocatalytic reaction so as to improve the catalytic rate. The Zn^{2+} doping concentration of 1,9% in the hollow sphere is also crucial, which is the highest concentration sample. The Zn^{2+} doping is on the surface of CuS lattice, because CuS is a typical P-type semiconductor, and Zn^{2+} forms a carrier trap on the surface, which can attract electrons to the interface of catalyst through charge recombination due to its positive potential. This results in a reduction in the energy required for electron-hole separation of the catalyst, which corresponds to our DRS results that the hollow spheres have a lower band gap (1,96 eV) than the normal pure CuS. The electron transfer increases the hole concentration of the hollow sphere catalyst, so in our capture experiment, the sample with AO (H + scavicant) has the most obvious reduction in catalytic efficiency. Hole h+ plays a leading role in the catalytic process of Zn^{2+}-doped CuS catalyst.

Conclusions

In conclusion, a green, simple and convenient photocatalyst synthesis process was designed in this study. CuS photocatalyst doped with Zn^{2+} ions was synthesized by one-step stirring in a low temperature water bath using green, non-toxic sodium thiosulfate as a sulfur source. The hollow spherical Zn^{2+} -doped CuS catalyst was prepared by adjusting the solvent ratio. Due to its large specific surface area and special fractional pores, the hollow spherical morphology provided more surface active sites for the adsorption of the catalyst and greatly improved the utilization efficiency of incident light. By doping Zn^{2+} ions to its lattice surface, the carrier trap is formed, which catalyzes hole extraction, promotes electron transition to the catalyst interface, reduces the activation energy of electron hole pairs, and significantly enhances the visible light response activity. Compared with the previously reported CuS series photocatalytic compounds, the photocatalytic activity of visible light is better, the reaction rate is 0,04736 min^{-1}, which is 12 times of that of common pure CuS, and the degradation efficiency can reach 65,6% after 5 cycles. It provides a more simple, green and efficient photocatalyst synthesis strategy compared with other reports, which has great application prospects in the field of photocatalysis.

REFERENCES

1. *Core-shell structure of sulphur vacancies*-CdS@CuS: Enhanced photocatalytic hydrogen generation activity based on photoinduced interfacial charge transfer / J. Guo, Y. Liang, L. Liu, J. Hu, H. Wang, W. An, W. Cui // J. Colloid Interface Sci. – 2021. – № 600. – P. 138–149.

2. *Preparation of flower-lik*e CuS/*reduced graphene oxide* (RGO) *photocatalysts for enhanced photocatalytic activity* / X.-S. Hu, Y. Shen, Y.-T. Zhang, J.-J. Nie // Journal of Physics and Chemistry of Solids. – 2017. – № 103. – P. 201–208.

3. *Flower-like* CuS/*graphene oxide with photothermal and enhanced photocatalytic effect for rapid bacteria-killing using visible light* / R. Lv, Y.-Q. Liang, Z.-Y. Li, S.-L. Zhu, Z.-D. Cui, S.-L. Wu // Rare Metals. – 2021. – Vol. 41, № 2. – P. 639–649.

4. *Rose-like* CuS *microflowers and their enhanced visible-light photocatalytic performance* / L. Zhao, L. Zhou, C. Sun, Y. Gu, W. Wen, X. Fang // CrystEngComm. – 2018. – Vol. 20, № 41. – P. 6529–6537.

5. *Efficient Self-Assembly Synthesis of Uniform* CdS *Spherical Nanoparticles-Au Nanoparticles Hybrids with Enhanced Photoactivity* / S. Han, L. Hu, N. Gao, A.A. Al-Ghamdi, X. Fang // Advanced Functional Materials. – 2014. – Vol. 24, № 24. – P. 3725–3733.

6. *Synthesis and optical properties of* CuS *nanoplate-based architectures by a solvothermal method* / F. Li, T. Kong, W. Bi, D. Li, Z. Li, X. Huang // Applied Surface Science. – 2009. – Vol. 255, № 12. – P. 6285–6289.

7. In_2S_3/CuS *nanosheet composite: An excellent visible light photocatalyst for* H_2 *production from* H_2S / A. Prakash, M. Dan, S. Yu, S. Wei, Y. Li, F. Wang, Y. Zhou // Solar Energy Materials and Solar Cells. – 2018. – № 180. – P. 205–212.

8. *Nanoporous CuS with excellent photocatalytic property* / W. Xu, S. Zhu, Y. Liang, Z. Li, Z. Cui, X. Yang, A. Inoue // Sci Rep. – 2015. – № 5. – P. 18125.

9. *Creating Carbon-Oxygen Bonds over* TiO_2 *Nanofibers for Synergistic Benefits of Visible-Light Response and Charge Separation toward Photocatalysis* / X. Xu, Y. Wang, R. Wang, J. Pan, J. Hu, H. Zeng // Advanced Materials Interfaces. – 2017. – Vol. 4, № 4.

10. *Uniform Zinc Oxide Nanowire Arrays Grown on Nonepitaxial Surface with General Orientation Control* / R. Zhu, W. Zhang, C. Li, R. Yang // Nano Lett. – 2013. – Vol. 13, № 11. – P. 5171-6.

11. *Zeinodin*, *R*. In-doped CuS nanostructures: Ultrasonic synthesis, physical properties, and enhanced photocatalytic behavior / R. Zeinodin, F. Jamali-Sheini // Physica B: Condensed Matter. – 2019. – № 570. – P. 148–156.

12. *Synthesis of* CuS *and* CuS/ZnS *core*/*shell nanocrystals for photocatalytic degradation of dyes under visible light* / U.T.D. Thuy, N.Q. Liem, C.M.A. Parlett, G.M. Lalev, K. Wilson // Catalysis Communications. – 2014. – № 44. – P. 62–67.

13. *Facile preparation and high capacitance performance of copper sulfide microspheres as supercapacitor electrode material* / T. Zhao, X. Peng, X. Zhao, J. Hu, W. Yang, T. Li, I. Ahmad // Composites Part B: Engineering. – 2019. – № 163. – P. 26–35.

14. *Ding*, *H*. Transformation of phase and heterojunction type by using HAc-adsorbed $Bi(NO_3)_3$ as a Bi source / H. Ding, H. Yu, Q. Han // J Colloid Interface Sci. – 2021. – № 604. – P. 429–440.

15. *Adhikari*, *S*. Hierarchical Design of CuS Architectures for Visible Light Photocatalysis of 4-Chlorophenol / S. Adhikari, D. Sarkar, G. Madras // ACS Omega. – 2017. – Vol. 2, № 7. – P. 4009–4021.

16. *Microwave-assisted controllable synthesis of hierarchical* CuS *nanospheres displaying fast and efficient photocatalytic activities* / H. Hu, J. Wang, C. Deng, C. Niu, H. Le // Journal of Materials Science. – 2018. – Vol. 53, № 20. – P. 14250–14261.

17. *Preparation and characterization of* CuS *hollow spheres* / Y. Huang, H. Xiao, S. Chen, C. Wang // Ceramics International. – 2009. – Vol. 35, № 2. – P. 905–907.

18. *Simmons*, *E.L*. Reflectance spectroscopy: application of the Kubelka-Munk theory to the rates of photoprocesses of powders / E.L. Simmons // Applied optics. – 1976. – Vol. 15, № 4. – P. 951-4.

19. *Tolvaj*, *L.* Validity limits of Kubelka–Munk theory for DRIFT spectra of photodegraded solid wood / L. Tolvaj, K. Mitsui, D. Varga // Wood Science and Technology. – 2010. – Vol. 45, № 1. – P. 135–146.

20. *Fast and simple approach for production of antibacterial nanocellulose/cuprous oxide hybrid films* / O.L. Evdokimova, M.E. Belousova, A.V. Evdokimova, T.V. Kusova, A.E. Baranchikov, K.S. Antonets, A.A. Nizhnikov, A.V. Agafonov // Cellulose. – 2021. – Vol. 28, № 5. – P. 2931–2945.

21. *Rapid toxicity elimination of organic pollutants by the photocatalysis of environment-friendly and magnetically recoverable step-scheme* $SnFe_2O_4$/$ZnFe_2O_4$ *nano-heterojunctions* / J. Wang, Q. Zhang, F. Deng, X. Luo, D.D. Dionysiou // Chemical Engineering Journal. – 2020. – № 379.

22. *Visible Light Photocatalytic* H_2*-Production Activity of* CuS/ZnS *Porous Nanosheets Based on Photoinduced Interfacial Charge Transfer* / J. Zhang, J. Yu, Y. Zhang, Q. Li, J.R. Gong // Nano Lett. – 2011. – Vol. 11, № 11. – P. 4774-9.

23. *Yang*, *D*. Revealing the role of surface elementary doping in photocatalysis / D. Yang, Z. Wang, J. Chen // Catalysis Science & Technology. – 2022. – Vol. 12, № 11. – P. 3634–3638.

24. *Effect of the counter ions on composition and morphology of bismuth oxyhalides and their photocatalytic performance* / Q. Han, K. Zhang, J. Zhang, S. Gong, X. Wang, J. Zhu // Chemical Engineering Journal. – 2016. – № 299. – P. 217–226.

25. *Mousavi*, *M*. Fabrication of novel magnetically separable nanocomposites using graphitic carbon nitride, silver phosphate and silver chloride and their applications in photocatalytic removal of different pollutants using visible-light irradiation / M. Mousavi, A. Habibi-Yangjeh, M. Abitorabi // J. Colloid Interface Sci. – 2016. – № 480. – P. 218–231.

26. *Origin of Photocatalytic Activation of Silver Orthophosphate from First-Principles* / X. Ma, B. Lu, D. Li, R. Shi, C. Pan, Y. Zhu // The Journal of Physical Chemistry C. – 2011. – Vol. 115, № 11. – P. 4680–4687.

27. *Zahid*, *A.H*. Highly stable 3D multilayered nanoparticles-based β-Bi_2O_3 hierarchitecture with enhanced photocatalytic activity / A.H. Zahid, Q. Han, X. Jia, S. Li, H. Hangjia, H. Liu // Optical Materials. – 2020. – № 109.

28. *In situ co-pyrolysis fabrication of* CeO_2/g-C_3N_4 *n-n type heterojunction for synchronously promoting photo-induced oxidation and reduction properties* / N. Tian, H. Huang, C. Liu, F. Dong, T. Zhang, X. Du, S. Yu, Y. Zhang // Journal of Materials Chemistry A. – 2015. – Vol. 3, № 33. – P. 17120–17129.

This study was supported by the Intergovernmental Cooperation Projects in the National Key Research and Development Plan of the Ministry of Science and Technology of PRC (No. 2022YFE0196800).

The article was submitted 14.11.2022.

Information about the authors

Gaopeng Yang – Master's Student of School of Chemical Engineering

Tiantian Wu – Master's Student of School of Chemical Engineering

Jingoing Cao – Ph. D., Lecturer

Xiaohong Jiang – Professor